The Astrophysical Journal, 868:66 (10pp), 2018 November 20 https://doi.org/10.3847/1538-4357/aae845

Helicity Removal and Coronal Fe XII Stalks: Evidence That the Axial Field Is Not Ejected but Resubmerged

Y.-M. Wang[1] and M. A. Berger[2]
[1] Space Science Division, Naval Research Laboratory, Washington, DC 20375, USA; yi.wang@nrl.navy.mil
[2] Centre for Geophysical and Astrophysical Fluid Dynamics, University of Exeter, Exeter, UK; m.berger@exeter.ac.uk
Received 2018 September 6; revised 2018 October 11; accepted 2018 October 12; published 2018 November 21

Abstract

The magnetic/current helicity of the coronal field is closely associated with the presence of a nonpotential axial component directed along the photospheric polarity inversion line (PIL), which is also the source of the axial/toroidal field in flux ropes and coronal mass ejections (CMEs). To better understand the role of this axial component in the evolution of coronal helicity, we use Fe XII 19.3 nm images and longitudinal magnetograms from the *Solar Dynamics Observatory* to track active regions (ARs) and their filament channels as they decay due to flux transport processes. We find that the Fe XII loop legs or "stalks," initially oriented almost perpendicular to the PIL, become closely aligned with it after ~1–4 rotations; this alignment is attributed to the progressive cancellation of the transverse field component at the PIL. As the AR flux continues to decay, the PIL becomes ever more distorted and the directions of the stalks are increasingly randomized. These observations suggest that most of the original axial field in ARs is not expelled in CMEs, but instead pinches off after the eruptions and becomes concentrated at the PIL. Because the twist of the field decreases, however, the helicity itself decreases, with CMEs removing a significant fraction of it in the form of disconnected flux ropes. Like most of the AR flux, the bulk of the axial field is eventually canceled/resubmerged, brought to the equator by the subsurface meridional flow, and annihilated (along with the remaining helicity) by merging with its opposite-handed counterpart from the other hemisphere.

Key words: Sun: activity – Sun: corona – Sun: coronal mass ejections (CMEs) – Sun: filaments, prominences – Sun: heliosphere – Sun: magnetic fields

1. Introduction

The solar magnetic field, in the form of sunspots, active regions (ARs), coronal arcades, filaments and their channels, and coronal mass ejections (CMEs), exhibits a nonpotential twist that tends to have opposite senses in the two hemispheres (for a review, see Pevtsov et al. 2014). The twist may be expressed mathematically in terms of the magnetic helicity, which is approximately conserved under dissipative processes (including, in particular, field-line reconnection) and is given by $H_{\rm m} = \int \boldsymbol{A} \cdot \boldsymbol{B} dV$, where $\boldsymbol{A}$ is the magnetic vector potential, $\boldsymbol{B} = \boldsymbol{\nabla} \times \boldsymbol{A}$ is the magnetic field, and the integral is over the volume enclosing the field. (If field lines cross the boundary of the volume, the helicity is measured relative to a potential field having the same boundary flux distribution.) Although not conserved, the current helicity $H_{\rm c} = \int \boldsymbol{J} \cdot \boldsymbol{B} dV$ is sometimes used as a proxy for the magnetic helicity, being somewhat easier to measure and interpret (see, e.g., Seehafer 1990). The hemispheric rule then states that $\boldsymbol{J} \cdot \boldsymbol{B} < 0$ (negative/left-handed helicity) predominates in the northern hemisphere, whereas $\boldsymbol{J} \cdot \boldsymbol{B} > 0$ (positive/right-handed helicity) predominates in the southern hemisphere.

The magnetic/current helicity observed in the corona is closely associated with the presence of a nonpotential field component directed along the polarity inversion line (PIL) of the photospheric field. This "axial" component gives rise to the shear in coronal arcades, to filament channels and filaments aligned with the PIL, and to the axial/toroidal component of flux ropes and CMEs. Roughly, for an isolated flux system, $H_{\rm m} \sim \Phi^2(T + W)$, where Φ denotes the total axial flux, T is the number of turns undergone by the twisted/poloidal component about the axis, and W represents the writhe of the axis.

The origin of the helicity and the hemispheric rule remains poorly understood. In general, helicity may be injected from below or it may be generated by horizontal motions on the solar surface (Berger & Field 1984; Chae 2001; Démoulin & Berger 2003). That the twist may originate beneath the surface or during the process of flux emergence is suggested by the superpenumbral whorls around sunspots, which (traced inward) form counterclockwise (clockwise) patterns in the northern (southern) hemisphere (Hale 1925; Richardson 1941). Correspondingly, AR loop systems tend to form backward-S (forward-S) structures in the northern (southern) hemisphere (see, e.g., Rust & Kumar 1996; Pevtsov et al. 1997; Lim & Chae 2009). On the other hand, it has also been recognized that the photospheric differential rotation, acting on a bipolar magnetic region (BMR) with a north–south oriented PIL, will generate helicity whose sign agrees with the hemispheric rule (van Ballegooijen et al. 1998; DeVore 2000). As pointed out by Pevtsov et al. (2014), however, a major difficulty with models that rely mainly on surface differential rotation (or on the Coriolis force) is that they would entail a strong latitudinal dependence of the helicity, which is not observed. (In particular, it may be difficult to account for filament channels that run along the equator, or those that encircle the polar caps, where the direction of rotational shearing would be opposite to that implied by the hemispheric rule.) Moreover, the helicity injected by rotational shearing of AR fields is generally found to be much smaller than that estimated to be present in magnetic clouds (see, e.g., Démoulin et al. 2002; van Driel-Gesztelyi & Green 2015). It is therefore likely that the bulk of the coronal helicity is transported from below with the emerging AR, a possible generation mechanism being deformation of the flux tubes by vortical turbulent motions in

the convection zone (Longcope et al. 1998; Berger & Ruzmaikin 2000).

Because it is conserved, the magnetic helicity injected into the corona from beneath the surface or by footpoint shearing would accumulate indefinitely unless it is ejected into the heliosphere or resubmerged. According to mean-field dynamo models, the buildup of subsurface helicity would quench the α effect, so that it must be expelled (see, e.g., Brandenburg et al. 2009). It is now widely accepted that CMEs are the primary mechanism for removing helicity from the Sun (see, e.g., Rust 1994; Low 1996; Démoulin et al. 2002; Nindos et al. 2003; Zhang & Low 2005; van Driel-Gesztelyi & Green 2015; Pariat et al. 2017; Patsourakos & Georgoulis 2017).

Here we describe *Solar Dynamics Observatory* (*SDO*) observations that confirm the tendency for AR fields to become increasingly aligned with the PIL as they decay, and discuss how this alignment can be reconciled with the removal of helicity by CMEs. We argue that, even though the axial field component determines the sign of the helicity, it evolves in a manner different from the helicity itself, eventually being resubmerged by flux cancellation rather than being ejected in CMEs. Any residual helicity not removed by CMEs is likewise retracted below the solar surface.

2. Fe XII Stalks as Indicators of the Axial Field Component

Since mid-2010, the Atmospheric Imaging Assembly (AIA) on *SDO* has been recording full-disk images in Fe XII 19.3 nm (among other extreme-ultraviolet and UV channels) with $0\farcs6$ pixels at a rate of once every 12 s. The Helioseismic and Magnetic Imager (*SDO*/HMI) provides full-disk line-of-sight magnetograms with $0\farcs5$ pixels once every 45 s. Sheeley et al. (2013; see also Wang et al. 2013) have described a procedure for deducing the chirality/handedness of filament channels using the 19.3 nm images. It was noted that, as ARs decay, the legs or "stalks"[3] of the loops rooted next to the PIL tend to bend leftward or rightward as they approach the PIL. Leftward bending signifies loop arcades with positive/right-handed helicity; rightward bending indicates negative/left-handed helicity.

Our focus here is on the long-term evolution of the Fe XII stalks. We present below some examples that illustrate how the axial field component remains present, and indeed dominates, when ARs are in late stages of decay.

2.1. Decay of a Large AR

Figure 1 shows the evolution of NOAA 12422, which emerged at latitude $L \sim -20°$ in late 2015 September. Allowing for additional flux injection by small neighboring ARs during October and December, the decay of this large AR can be tracked for a period as long as ~9 rotations. The Fe XII loops are initially oriented almost perpendicular to the PIL (see Figure 1(a), where the sunspot fields are still in the process of emerging on September 27), and remain so even after one 27 day rotation (October 24: Figure 1(b)). However, after two rotations (2015 November 20: Figure 1(c)), the stalks have begun to line up with the PIL, bending sharply leftward as they approach it from either side. The positive/right-handed helicity of the loop system is characteristic of southern-hemisphere ARs.[4] The Fe XII stalks reach their state of closest alignment with the PIL during 2016 January–February, some ~4 rotations after the AR emerged (Figures 1(d)–(e)). Subsequently, the PIL and filament channel become increasingly distorted, both because of the intermingling of opposite-polarity flux elements due to supergranular convection and because of nearby flux emergence. By late May (Figure 1(h)), the directions of the stalks appear to have been largely randomized over most of the original channel.

2.2. Decay of a Small AR

NOAA 12699, centered at $L \sim -7°$, is shown in Figure 2(a) just before it undergoes an eruption early on 2018 February 12. As the AR flux spreads and cancellation proceeds at the PIL, the orientation of the Fe XII stalks relative to the PIL changes from roughly perpendicular to strongly aligned, with maximal alignment being attained after ~2 rotations (April 6: Figure 2(c)). The leftward bending of the stalks corresponds to positive helicity and is consistent with the hemispheric rule and with the forward-S topology of the original AR. (At the end of March, a small BMR emerged at the western edge of the decaying region, reinforcing the positive-polarity leading sector as seen in the April 6 frame.) By May 3 (Figure 2(d)), the PIL has become considerably less well defined due to the continued intermingling of opposite-polarity flux elements; correspondingly, the orientation of the stalks begins to approach a quasi-random state.

2.3. Formation and Decay of a Circular Filament Channel

Figure 3 shows the evolution of NOAA AR 11641 over three 27 day rotations, spanning the interval from 2013 January 3 to March 25. This small AR, centered at latitude $L \sim +5°$, has the form of a bipole with a negative-polarity leading sector, which matches the dominant polarity of the surrounding region. On January 3, a few days after the emergence of the BMR, the loops connecting its poles are oriented almost perpendicular to the PIL (Figure 3(a)). One rotation later (Figure 3(b)), a circular filament channel has formed around the positive-polarity sector of the BMR. Since the Fe XII stalks curve toward the right as they approach the PIL, the loop arcade has the negative/left-handed helicity characteristic of northern-hemisphere filament channels. The inferred chirality is also consistent with the counterclockwise spiral seen around the positive-polarity sector of the AR on January 3. It is evident that this rapid alignment of the Fe XII stalks with the circular, near-equatorial PIL cannot be the result of photospheric differential rotation alone. Instead, the cancellation of the formerly dominant transverse field component at the PIL has apparently acted to unmask the preexisting axial field component.

During the next two rotations (Figures 3(c) and (d)), the circular PIL becomes increasingly convoluted as supergranular convective motions continue to mix the positive- and negative-polarity flux elements. By March 25 (Figure 3(d)), it has

[3] Sheeley et al. (2013) refer to these structures as "cells" because of their circular appearance when viewed along their axes. However, when used to infer chirality, the loop legs are viewed at an angle and appear as elongated stalks with bulbous bases.

[4] In Figures 1(b) and (c), some of the loops on the north side of the AR appear to spiral inward in the counterclockwise rather than the clockwise sense, suggesting that the direction of whirl (which also depends on the current-free contribution to the field) is not always a reliable indicator of handedness.

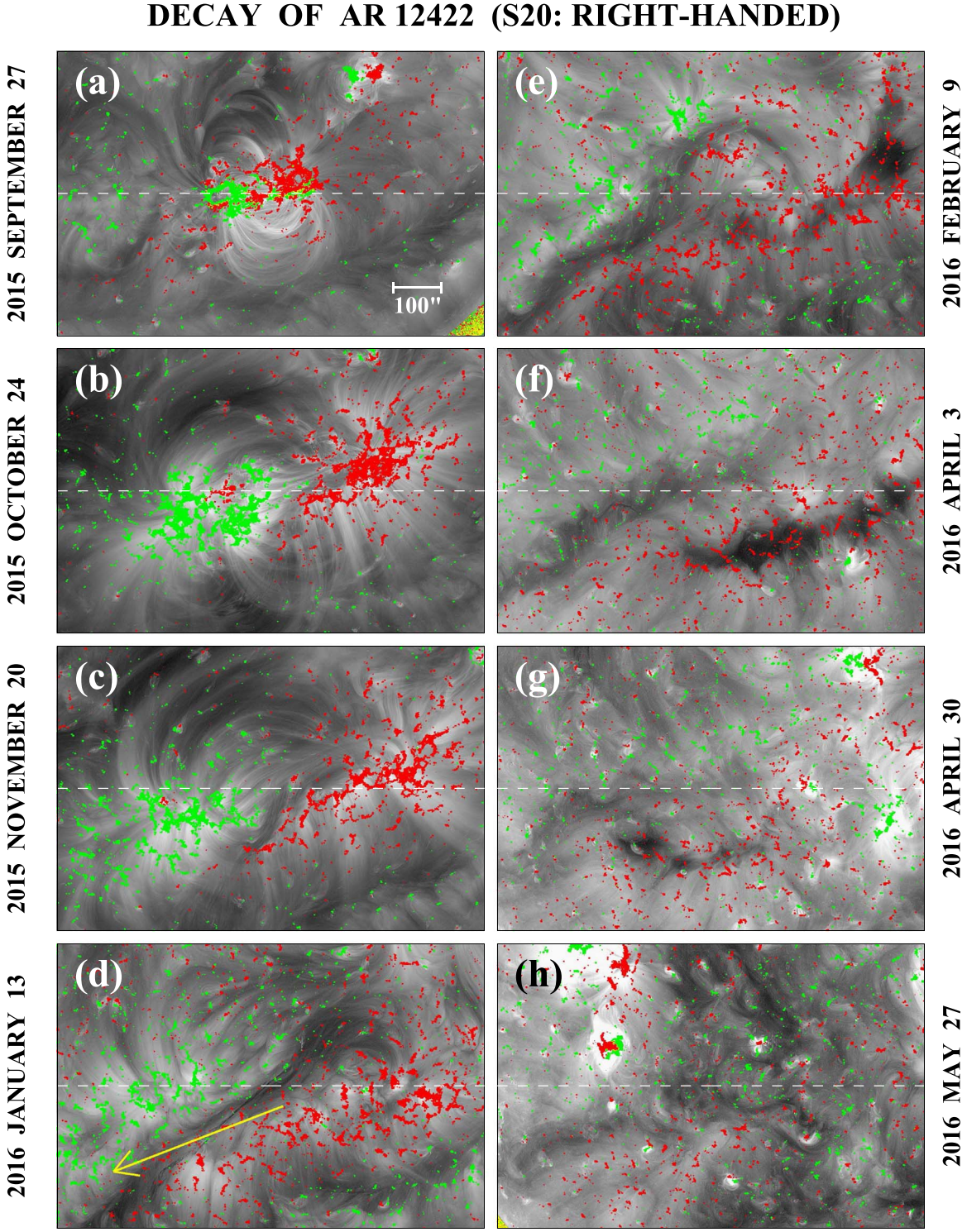

Figure 1. The evolution of NOAA 12422, which emerged at latitude $L \sim -20^\circ$ in 2015 September, is tracked over a period of nine 27 day rotations. Here and in subsequent figures, each frame shows a sharpened, one-minute average of Fe XII 19.3 nm images recorded at 23:00 UTC on the given day; contours of the HMI line-of-sight photospheric field $B_{\rm los}$ are superposed, with red (green) indicating positive (negative) polarity. In (a), the AR is still in the process of emerging, with its loops expanding in the direction transverse to the PIL. One rotation later (b), the loops remain almost perpendicular to the PIL. The yellow arrow in (d) indicates the direction of the axial field on 2016 January 13, by which time the Fe XII stalks have become closely aligned with the PIL (due to the cancellation of the transverse field component); the leftward bending of the stalks signifies positive helicity. As the PIL becomes more convoluted ((g) and (h)), the stalks become increasingly randomized in direction and the axial field component begins to undergo flux cancellation. White dashed line marks the location of latitude -20°. The contours of $B_{\rm los}$ have been saturated at ± 100 G in (a)–(c) and at ± 50 G in (d)–(h).

become difficult to identify any coherent PIL or filament channel, and the directions of the stalks appear to be largely randomized.

2.4. ARs with Dual Helicities

Figures 4(a)–(c) show the decay of NOAA 12645, which emerged at $L \sim -10^\circ$ near the end of 2017 March. Again,

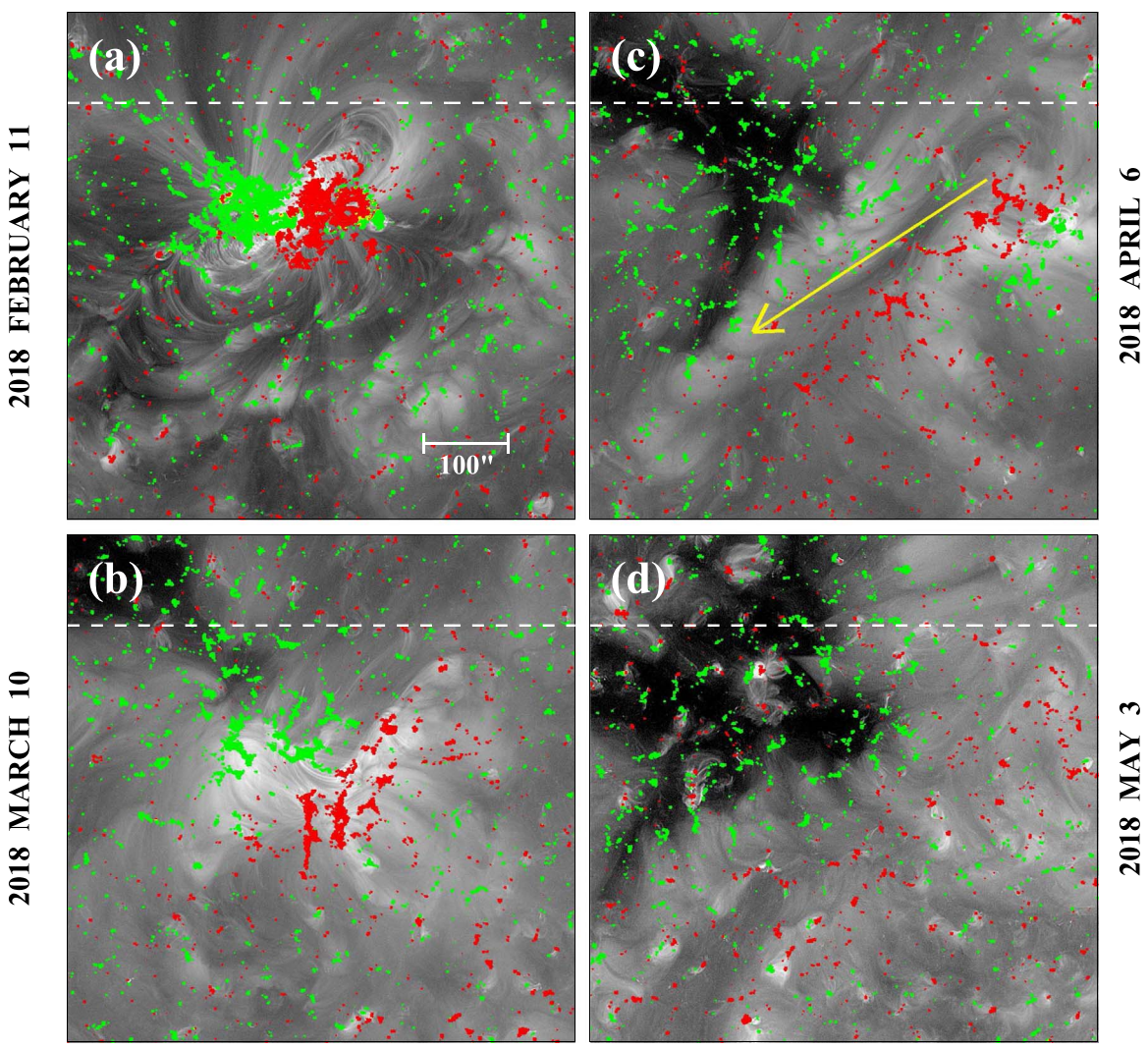

Figure 2. The evolution of NOAA 12699, centered at $L \sim -7°$, is tracked during 2018 February–May. Here and in the following figures, the white dashed line marks the equator. In (a), the new AR is shown at 23:00 UTC on February 11, just before it undergoes an eruption at the start of February 12. After two rotations (c), the leftward-bending Fe XII stalks reach their state of closest alignment with the PIL; the arrow indicates the direction of the axial field within the channel. (Some new flux has emerged on the northwest side of the decaying AR remnant.) By the next rotation (d), however, the stalks have become misaligned as the opposite-polarity flux elements continue to mix. (The dark area to the northeast of the filament channel is a negative-polarity coronal hole.) The contours of B_{los} are saturated at ± 50 G, with red (green) denoting positive (negative) polarity.

the loops are initially oriented almost transverse to the PIL. During subsequent rotations, the photospheric flux spreads both southeastward and toward the equator, forming a backward-C PIL bisected by loops that cross the PIL at right angles. The Fe XII stalks rooted to the north (south) of the "bisector" bend to the right (left) as they approach the PIL. The two sectors thus have opposite helicities: negative on the equatorward side of the AR but positive (as is normal for the southern hemisphere) farther to the south.

As another example of opposite helicities appearing during the decay of an AR, Figures 4(d)–(f) display the evolution of NOAA 12672, which emerged at $L \sim +7°$ during 2017 August. Again, as the BMR flux spreads, the PIL separates into a northern branch where the adjacent Fe XII stalks curve to the right (corresponding to negative helicity) and a southern branch where they curve to the left (corresponding to positive helicity). As in the first example, the two sectors are divided by a transverse stalk (compare Figures 4(b) and (e)).

A third case is displayed in Figures 4(g)–(i), which shows the evolution of NOAA 12712 ($L \sim +15°$) during 2018 May–August. Even though the AR emerged well north of the equator, the stalks on the equatorward side of its trailing-polarity sector bend leftward along the PIL, signifying that the filament channel locally has positive helicity. In contrast, the stalks rooted northward of the "bisector" bend rightward, as expected for a northern-hemisphere AR.

These three examples involve ARs that emerged toward the end of solar cycle 24 and were located at relatively low latitudes; in every case, moreover, the stalks rooted on the equatorward side of the AR showed the handedness characteristic of the opposite hemisphere. A possible explanation for the dual helicities is that the background flux on the equatorward side of the AR originates from the other hemisphere and is sufficiently strong to determine the local helicity sign. This is certainly true in the case of NOAA 12650, displayed in Figure 5. Here, a series of PIL-aligned,

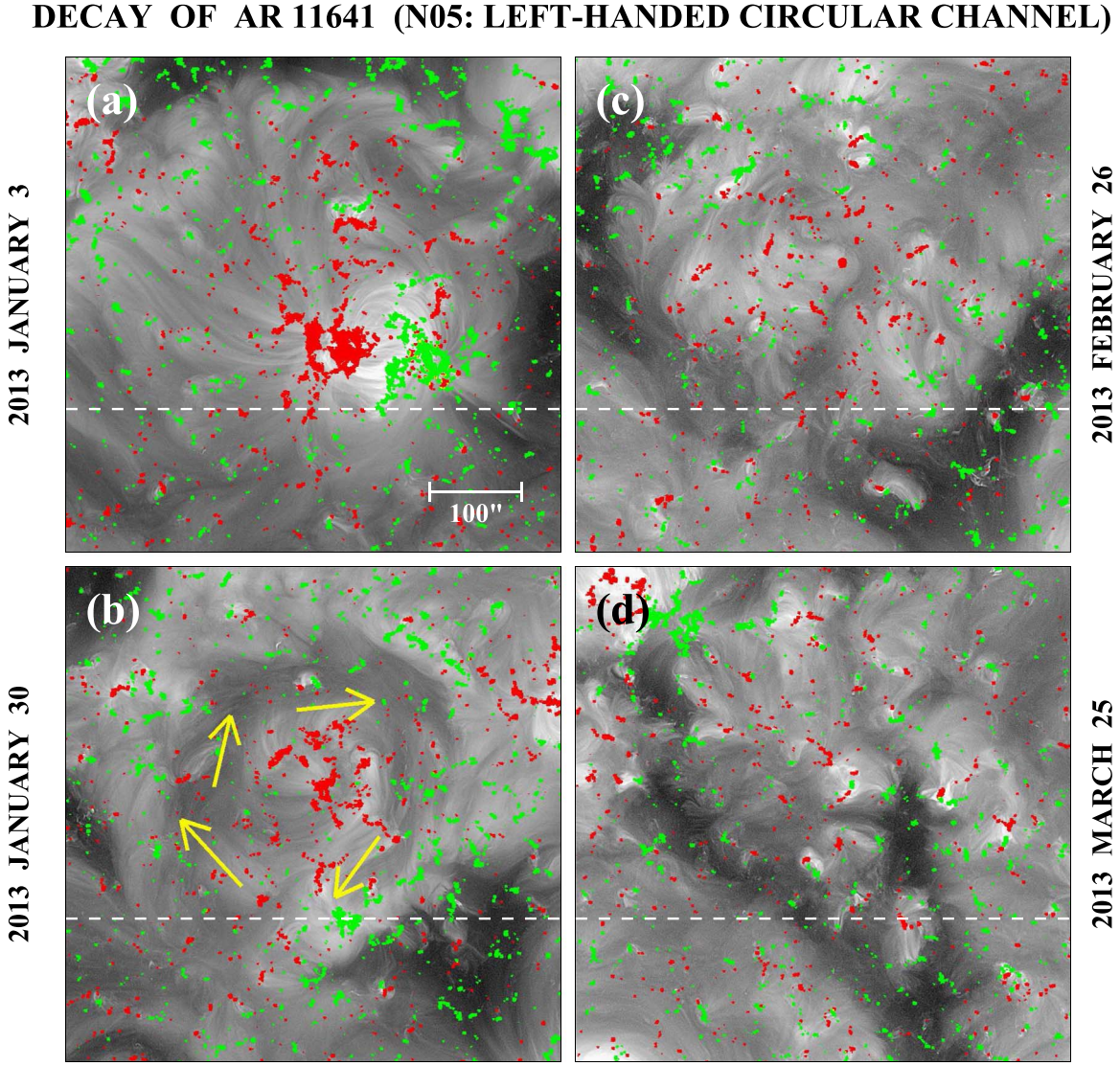

Figure 3. Formation and decay of a circular filament channel around the trailing sector of NOAA 11641, 2013 January–March. White dashed line marks the equator. As shown in (a), the AR emerged at $L \sim +5°$ in a predominantly negative-polarity background. One rotation later (b), a circular channel has formed around the positive-polarity sector of the BMR. Arrows indicate the direction of the axial field; the rightward curving of the stalks signifies negative helicity and is consistent with the counterclockwise whorl around the trailing pole on January 3. During the next two rotations ((c) and (d)), the opposite-polarity flux elements become increasingly mixed and the channel becomes poorly defined. (The dark areas lying outside the channel are negative-polarity coronal holes.) The contours of B_{los} are saturated at ± 50 G, with red (green) denoting positive (negative) polarity.

leftward-bending Fe XII stalks is seen to be already present on the south side of the AR when it emerged at $L \sim +8°$ during 2017 April (Figure 5(a)). One rotation later (Figure 5(b)), a "bisector" stalk separates this positive-helicity channel from the rightward-bending stalks that have formed along the internal PIL of this northern-hemisphere AR, which evidently has intrinsic negative helicity.

It appears that the hemispheric rule is often violated over a wide latitudinal band around the equator, particularly during the later years of the sunspot cycle (see also Hagino & Sakurai 2005; Hao & Zhang 2011). These violations may be associated not only with ARs that emerge on the "wrong" side of the equator,[5] but also with the diffusive transport of decaying AR flux into the opposite hemisphere.

[5] Examples of large ARs that disobeyed the hemispheric rule during 2017 include NOAA 12651–52 ($L \sim +12°$) and NOAA 12682 ($L \sim -9°$).

3. How is the Axial Field Component Removed?

The (nonpotential) field component along the PIL is a fundamental constituent of AR helicity, determining both its sign and its associated flux. The observations described above indicate that this axial field remains present, and indeed becomes dominant, long (~1–6 rotations) after the emergence of the AR, before eventually decaying away. The lag between the emergence phase and the alignment of the stalks with the PIL reflects the time required for flux cancellation at the PIL to strip away the transverse field component, the same process that may be responsible for the formation of filaments and filament channels (see, e.g., van Ballegooijen & Martens 1989; Zirker et al. 1997; van Ballegooijen et al. 1998, 2000; Mackay & Gaizauskas 2003; Wang & Muglach 2007; Martin et al. 2008; Yeates & Mackay 2009; Litvinenko 2010; Mackay et al. 2010). Here, the main role of the photospheric differential rotation is not to generate helicity by shearing the coronal loops

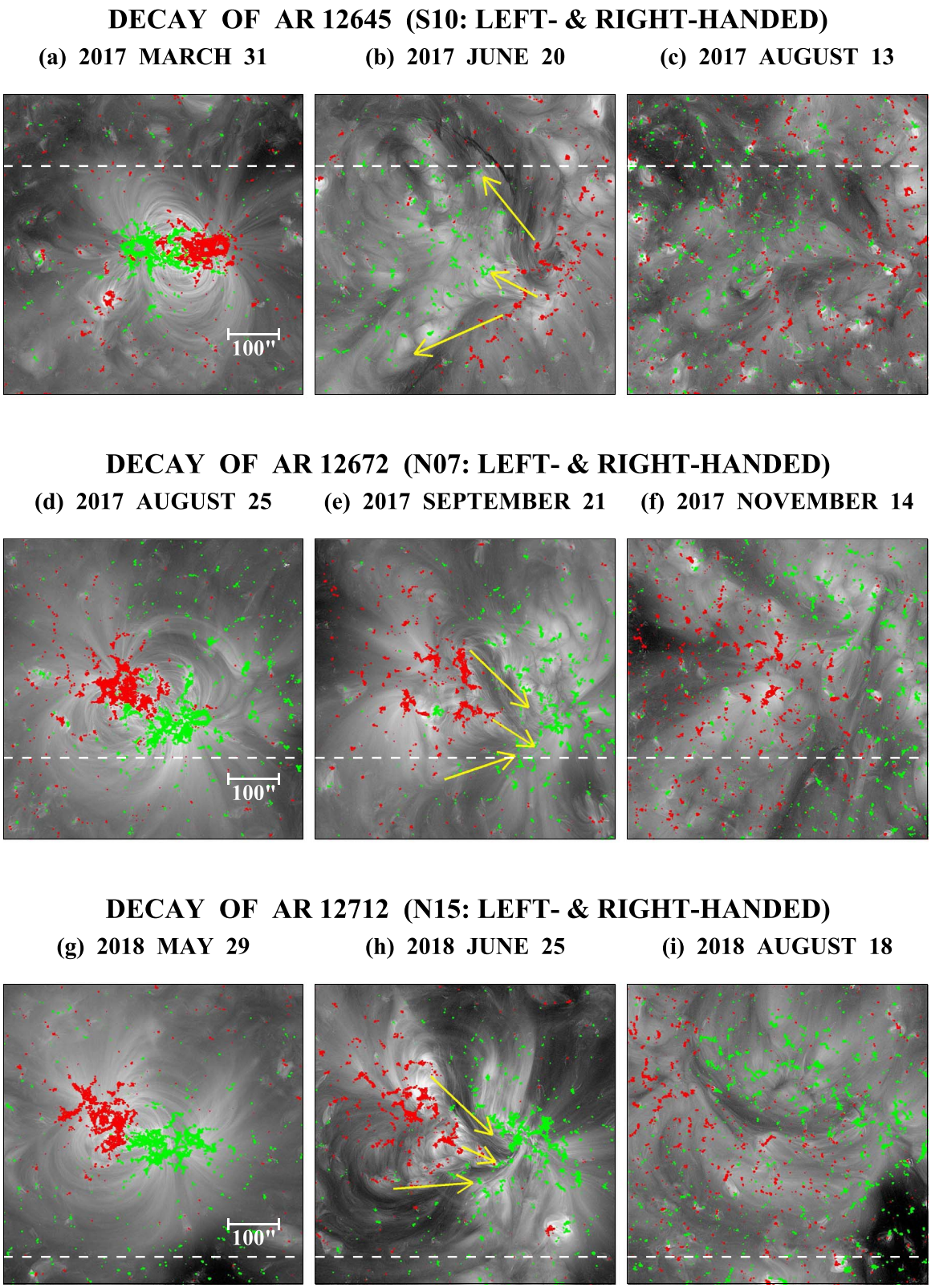

Figure 4. Low-latitude ARs with dual helicity. White dashed line marks the equator, while yellow arrows indicate the direction of the axial field component. (a)–(c) NOAA 12645, which emerged at $L \sim -10^{\circ}$ during 2017 March. As seen on June 20, the Fe XII stalks rooted along the southern segment of the PIL bend leftward (corresponding to positive helicity), whereas those rooted along the northern/equatorward segment bend rightward (corresponding to negative helicity); the two halves of the filament channel are divided by a stalk that crosses the PIL at right angles. (d)–(f) NOAA 12672, which emerged at $L \sim +7^{\circ}$ during 2017 August. (g)–(i) NOAA 12712, which emerged at $L \sim +15^{\circ}$ during 2018 May. In all cases, the stalks bend rightward to the north of the "bisector," but leftward to the south of it.

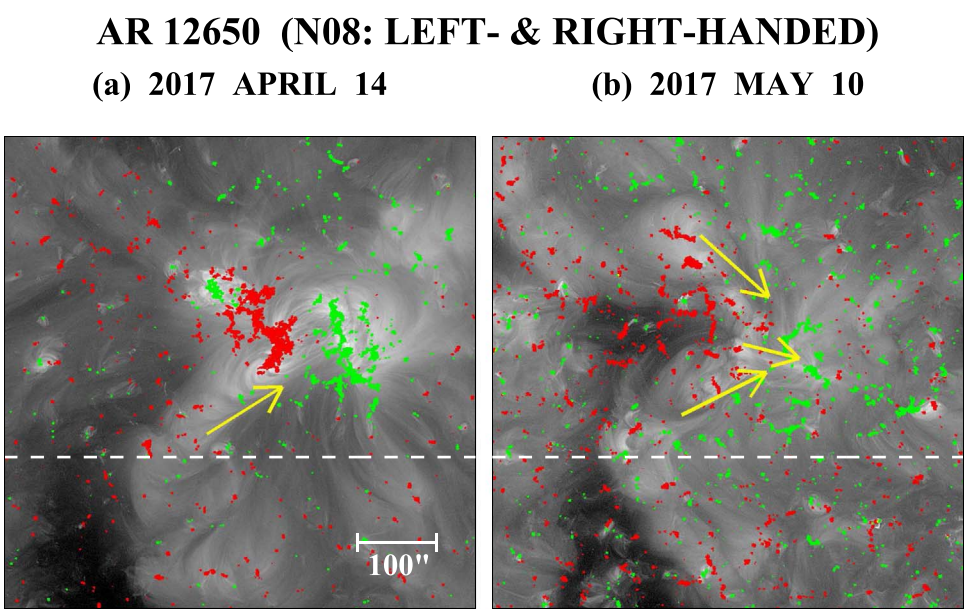

Figure 5. Formation of a filament channel with dual helicity. Dashed line marks the equator; arrows indicate the direction of the axial field. (a) NOAA 12650, centered at $L \sim +8°$, emerges just northward of a background PIL with leftward-pointing Fe XII stalks. (b) After one rotation, rightward-pointing stalks have formed along the internal PIL of the AR, which are separated from the leftward-pointing background stalks by a perpendicular "bisector."

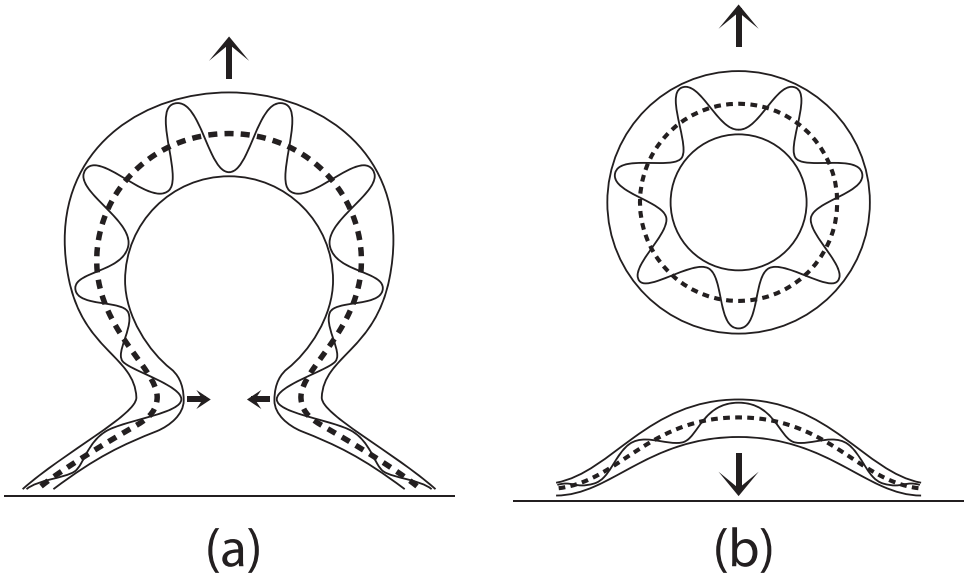

Figure 6. Schematic illustration of a CME event in which helicity but not the axial field component is removed. (a) The CME initially has the form of a flux rope with a poloidal component winding around a semicircular toroidal axis, which in turn represents the erupting axial field of the underlying AR. As the eruption proceeds, the opposite-polarity legs of the flux rope converge, eventually reconnecting and pinching off. (b) The ejected ring of twisted flux carries a net helicity $H_m \sim \Phi^2 T$, where Φ is the amount of axial flux threading the original flux rope and T is the number of winds around the ring. The pinched-off legs of the flux rope contain the same total flux Φ as the pre-eruption axial field, but the structure now has fewer winds and thus less helicity than the original flux rope.

themselves (DeVore 2000), but to expedite the mixing and cancellation of opposite-polarity flux elements by continually stretching/lengthening the PIL.

It is widely agreed that CMEs act to remove helicity from the Sun (see, e.g., the review of Zhang & Low 2005). Since eruptive events like CMEs and flares tend to occur early during the lifetime of an AR, the question arises as to how a strong axial field component can remain present so long into the decay phase of the AR, when this component is closely associated with the helicity that is expelled into the heliosphere.

To answer this question, let us consider an idealized CME represented by a semicircular flux rope with both legs rooted in the photosphere (Figure 6(a)). The toroidal component of the flux rope is formed from the underlying axial field along the PIL, while the poloidal component (if not originally present) is formed by pinching off the coronal loops oriented transverse to the PIL. If the flux rope travels outward through the heliosphere while remaining attached to the Sun, the legs will become radially aligned and the axial component will be converted into open flux. In that case, the post-eruption arcade should be less skewed than its pre-eruption counterpart. In addition, long-lived dark areas/coronal holes should form at the footpoints of the flux rope; these, however, are generally not observed.

An alternative possibility is that the legs of the flux rope converge and pinch off, causing the axial field to collapse back onto the Sun and a ring of twisted flux to be ejected into the

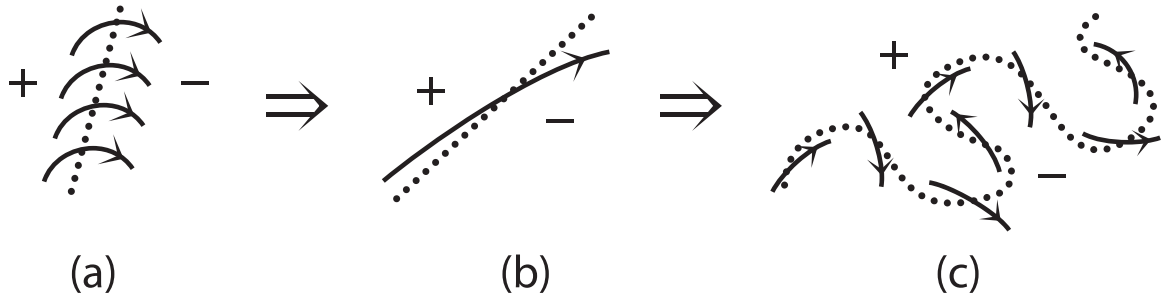

Figure 7. Removal of the axial field component by flux cancellation. Dotted lines mark the PIL, while solid lines with arrows show representative coronal field lines and their directions. (a) The arcade loops are initially oriented almost perpendicular to the PIL, while exhibiting a small skew corresponding to right-handed helicity. (b) The axial field component dominates after flux cancellation at the PIL has weakened the transverse field component. (The corresponding Fe XII stalks would bend leftward at the PIL.) (c) As the photospheric flux continues to disperse and the PIL becomes increasingly distorted, the coronal loops shorten and begin to take on random orientations. The axial field component then undergoes flux cancellation (submergence).

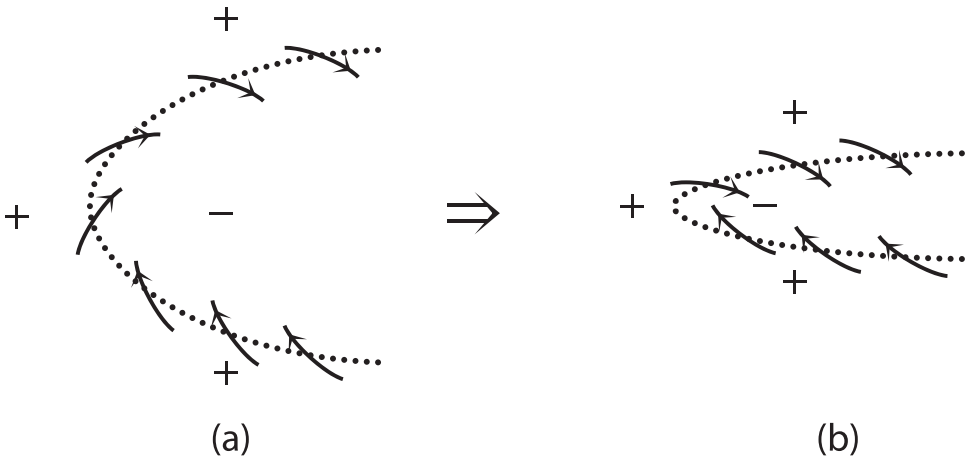

Figure 8. When a minority-polarity region contracts and disappears as a result of flux cancellation by the surrounding dominant polarity, the axial field along the PIL likewise disappears. (a)–(b) illustrate the evolution of a negative-polarity switchback surrounded by positive-polarity flux. A similar process might occur in a circular PIL that shrinks to a point and vanishes. In reality, the bulk of the filament channel field is probably again submerged together with its associated helicity, rather than being dissipatively annihilated at the surface.

heliosphere (Figure 6(b)). The post-eruption arcade would then remain skewed, while the dimmings at the endpoints of the flux rope would eventually disappear. Denoting the total flux threading the original flux rope by Φ, the helicity removed by the detached ring would be on the order of $H_{\rm m} \sim \Phi^2 T$, where T is the number of turns made by the poloidal field around the ring (and the contribution of writhe is neglected). The helicity of the post-eruption arcade decreases by a corresponding amount; since the axial flux remains the same as before, the decrease must occur in the nonpotential twist (and/or writhe) of the loop system.

The second possibility is consistent with the long-term evolution of the Fe XII stalks, as well as with the limited lifetimes of the transient coronal holes observed in the wake of CMEs, which typically disappear within ~1–2 days. We therefore conclude that, even though CMEs help to rid the Sun of helicity, they do not remove the axial field component, which must be disposed of by other means.

The case studies of Section 2 suggest that the Fe XII stalks reach a state of maximum alignment with the PIL after a few rotations, but that their directions then become progressively randomized as the opposite-polarity flux elements continue to mix and the PIL becomes increasingly distorted (see Figure 7). When the flux distribution begins to take on a salt-and-pepper appearance and the PIL no longer has a well-defined direction, the distinction between the transverse and axial field components is lost; both components then undergo flux cancellation. By this time, the large-scale Fe XII structures have been replaced by short loops with closely spaced footpoints. As pairs of opposite-polarity footpoints converge in the supergranular flow field, the loops are pulled below the surface by magnetic tension.

During the period when the stalks are PIL-aligned, net helicity remains present in the form of the mutual helicity between the axial field inside the filament cavity and the transverse field in the overlying streamer.[6] Some of this helicity is expelled in filament eruptions, while the rest is eventually resubmerged.

Although the photospheric turbulent convection converts the long Fe XII stalks into small, quasi-randomly oriented loops that are retracted below the surface, this process does not necessarily result in the dissipative annihilation of the axial field component. Unless the mixing occurs on both large and small scales, the canceled/resubmerged field is likely to retain some of its original large-scale organization. The subsurface field will then have a net axial component that is oppositely directed in the two hemispheres. The axial field might in principle be annihilated by surface transport processes in the

[6] As discussed by Martin (1998), the intermediate legs or "barbs" of filaments, which appear to be rooted in minority-polarity flux on the "wrong" side of the PIL, have chirality opposite to that of the overlying coronal loops. This effect may reduce the net helicity of the cavity-streamer system.

case of a circular PIL or switchback (Figure 8), if the PIL encloses minority-polarity flux that is completely canceled by the surrounding dominant polarity. Even here, however, the actual dissipation timescales may be sufficiently long that the bulk of the filament channel field with its associated helicity is submerged during flux cancellation, instead of being annihilated at the surface.

In the flux transport dynamo (see the review of Charbonneau 2010), meridional circulation continually advects the subsurface flux equatorward. We suggest that the resubmerged axial field is transported to the equator by the meridional flow, where it is then annihilated by merging with its opposite-hemisphere counterpart. The annihilation of the axial field also removes the resubmerged remnant helicity. This scenario for the evolution of the axial field is analogous to that proposed in Wang & Sheeley (1991) and Wang et al. (1991) for the evolution of the toroidal field in the flux transport dynamo. There, it was pointed out that the toroidal flux that emerges at the solar surface in the form of ARs is unlikely to be bodily expelled from the Sun, as assumed by Babcock (1961) and Leighton (1969). Instead, the bulk of it is eventually resubmerged via flux cancellation and annihilated at the equator.

4. Conclusions

The main point made in this paper is that the evolution of the axial field component in ARs differs from that of their helicity, even though this component determines the sign and magnitude of the helicity. Our arguments are based on the observed evolution of Fe XII stalks, which indicate the local direction of the coronal field. Our conclusions may be summarized as follows.

1. The axial (PIL-aligned) field component remains strongly present long after the emergence of the AR and after most of the AR-associated CMEs have occurred. As the transverse field is progressively canceled at the PIL, the axial field becomes increasingly dominant, with the Fe XII stalks becoming closely aligned with the PIL after ~1–4 rotations.[7]
2. Most of the axial field in CMEs pinches off after the eruption, rather than being converted into open flux. This inference is consistent with the absence of long-lived dimmings at the footpoints of flux-rope CMEs, as well as with the relative constancy of the interplanetary field strength over the solar cycle (see below).
3. Each CME removes net helicity H_m on the order of $\Phi^2 T$, where Φ is the axial/toroidal flux threading the pinched-off ejection and T is the number of turns associated with its poloidal component. The twist of the underlying field undergoes a corresponding decrease.
4. After reaching their state of maximum alignment with the PIL, the stalks gradually become randomized in direction as the PIL becomes increasingly convoluted. As the opposite-polarity flux elements continue to mix, the axial field undergoes flux cancellation and most of it is resubmerged.
5. The part of the axial field that is not dissipatively annihilated at the solar surface is carried to the equator by the subsurface meridional flow and merged with its oppositely directed counterpart from the other hemisphere.
6. The resubmerged fields may contain remnant helicity, which is annihilated at the equator along with the axial field on which its sign and magnitude depend.

The fate of the axial field component is analogous to that of the toroidal flux that emerges in the form of ARs: instead of being ejected from the Sun, both are resubmerged and eventually annihilated at the equator. Indeed, since the general tendency is for the direction of the PIL to evolve from north–south to east–west due to the photospheric differential rotation, the axial field will tend to change from a poloidal to a toroidal orientation as the AR decays. Conversely, the transverse field component (the bulk of which is canceled early during the decay phase) tends to evolve from "toroidal" to "poloidal."

Our conclusion that CMEs eventually disconnect from the Sun is an inference based on the observed evolution of filament channels. The presence of counterstreaming suprathermal electrons and the relative paucity of heat flux dropouts in interplanetary CMEs are sometimes interpreted as evidence against disconnection (see, e.g., Lin & Kahler 1992). However, this interpretation has been questioned by Owens & Crooker (2007) and Crooker & Pagel (2008), who argue that the low occurrence rate of heat flux dropouts may nevertheless be consistent with eventual disconnection or with reconnection between open and closed flux (see also McComas et al. 1992). If the pinched-off CME has the form of a flux rope that closes on itself (as in Figure 6(b)), it is not obvious that scattering will immediately isotropize the pitch angle distribution or cause the strahl to disappear, particularly if mechanisms exist for accelerating electrons in situ; magnetic mirroring of trapped electrons might also help to maintain a bidirectional heat flux. It is worth noting that, in their original analysis of bidirectional electron events, Gosling et al. (1987) favored an interpretation in terms of disconnected "plasmoids" rather than structures rooted at both ends in the Sun. An independent argument in favor of disconnection (see, e.g., McComas et al. 1989; Riley et al. 2004) is that the interplanetary field strength would otherwise build up indefinitely, instead of remaining roughly constant (to within a factor of order 2) over the solar cycle.

We are indebted to N. U. Crooker, B. Kliem, M. G. Linton, M. B. Moldwin, O. Panasenco, and S. Patsourakos for helpful discussions and correspondence. This work was funded by the Chief of Naval Research.

ORCID iDs

Y.-M. Wang https://orcid.org/0000-0002-3527-5958
M. A. Berger https://orcid.org/0000-0001-7633-3774

References

Babcock, H. W. 1961, ApJ, 133, 572
Berger, M. A., & Field, G. B. 1984, JFM, 147, 133
Berger, M. A., & Ruzmaikin, A. 2000, JGR, 105, 10481
Brandenburg, A., Candelaresi, S., & Chatterjee, P. 2009, MNRAS, 398, 1414
Chae, J. 2001, ApJL, 560, L95
Charbonneau, P. 2010, LRSP, 7, 3
Crooker, N. U., & Pagel, C. 2008, JGR, 113, A02106
Démoulin, P., & Berger, M. A. 2003, SoPh, 215, 203
Démoulin, P., Mandrini, C. H., van Driel-Gesztelyi, L., et al. 2002, A&A, 382, 650
DeVore, C. R. 2000, ApJ, 539, 944
Gosling, J. T., Baker, D. N., Bame, S. J., et al. 1987, JGR, 92, 8519

[7] Although the PIL-aligned field and the overlying streamer may each show little twist, their mutual helicity may continue to drive filament eruptions during this stage of the AR decay.

Hagino, M., & Sakurai, T. 2005, PASJ, 57, 481
Hale, G. E. 1925, PNAS, 11, 691
Hao, J., & Zhang, M. 2011, ApJL, 733, L27
Leighton, R. B. 1969, ApJ, 156, 1
Lim, E.-K., & Chae, J. 2009, ApJ, 692, 104
Lin, R. P., & Kahler, S. W. 1992, JGR, 97, 8203
Litvinenko, Y. E. 2010, ApJ, 720, 948
Longcope, D. W., Fisher, G. H., & Pevtsov, A. A. 1998, ApJ, 507, 417
Low, B. C. 1996, SoPh, 167, 217
Mackay, D. H., & Gaizauskas, V. 2003, SoPh, 216, 121
Mackay, D. H., Karpen, J. T., Ballester, J. L., Schmieder, B., & Aulanier, G. 2010, SSRv, 151, 333
Martin, S. F. 1998, SoPh, 182, 107
Martin, S. F., Panasenco, O., Engvold, O., & Lin, Y. 2008, AnGeo, 26, 3061
McComas, D. J., Gosling, J. T., Phillips, J. L., et al. 1989, JGR, 94, 6907
McComas, D. J., Gosling, J. T., & Phillips, J. L. 1992, JGR, 97, 171
Nindos, A., Zhang, J., & Zhang, H. 2003, ApJ, 594, 1033
Owens, M. J., & Crooker, N. U. 2007, JGR, 112, A06106
Pariat, E., Leake, J. E., Valori, G., et al. 2017, A&A, 601, A125
Patsourakos, S., & Georgoulis, M. K. 2017, SoPh, 292, 89
Pevtsov, A. A., Berger, M. A., Nindos, A., Norton, A. A., & van Driel-Gesztelyi, L. 2014, SSRv, 186, 285
Pevtsov, A. A., Canfield, R. C., & McClymont, A. N. 1997, ApJ, 481, 973
Richardson, R. S. 1941, ApJ, 93, 24
Riley, P., Gosling, J. T., & Crooker, N. U. 2004, ApJ, 608, 1100
Rust, D. M. 1994, GeoRL, 21, 241
Rust, D. M., & Kumar, A. 1996, ApJL, 464, L199
Seehafer, N. 1990, SoPh, 125, 219
Sheeley, N. R., Jr., Martin, S. F., Panasenco, O., & Warren, H. P. 2013, ApJ, 772, 88
van Ballegooijen, A. A., Cartledge, N. P., & Priest, E. R. 1998, ApJ, 501, 866
van Ballegooijen, A. A., & Martens, P. C. H. 1989, ApJ, 343, 971
van Ballegooijen, A. A., Priest, E. R., & Mackay, D. H. 2000, ApJ, 539, 983
van Driel-Gesztelyi, L., & Green, L. M. 2015, LRSP, 12, 1
Wang, Y.-M., & Muglach, K. 2007, ApJ, 666, 1284
Wang, Y.-M., & Sheeley, N. R., Jr. 1991, ApJ, 375, 761
Wang, Y.-M., Sheeley, N. R., Jr., & Nash, A. G. 1991, ApJ, 383, 431
Wang, Y.-M., Sheeley, N. R., Jr., & Stenborg, G. 2013, ApJ, 770, 72
Yeates, A. R., & Mackay, D. H. 2009, SoPh, 254, 77
Zhang, M., & Low, B. C. 2005, ARA&A, 43, 103
Zirker, J. B., Martin, S. F., Harvey, K., & Gaizauskas, V. 1997, SoPh, 175, 27